Short communication

Criterion for insertion-induced microcracking and debonding of thin films

Fuqian Yang*

Materials Program, Department of Chemical and Materials Engineering, University of Kentucky, Lexington, KY 40506, United States

ARTICLE INFO

ABSTRACT

The insertion of lithium into electric anode in a lithium-ion battery results in local volume expansion and creates compressive stress in materials. To relax the compressive stress, structural damage including microcracking and local buckling can occur. Using the theory of diffusion-induced stress and the energy principle, analytical relations between the critical concentration of solute atoms and average damage size are established for the insertion-induced cracking and buckling in an elastic film. Numerical results show that surface cracking will prevail over local buckling in accord with experimental observation. For local buckling of a given size, there exists a minimum critical concentration which is determined by the film thickness and the ratio of the Dupré constant to Young's modulus of the film.

© 2010 Elsevier B.V. All rights reserved.

1. Introduction

Lithium-ion batteries (LIBs) have the potential for use in hybrid electric vehicles and plug-in hybrid electric vehicles, which generally require a service life of more than 10 years under sustained electrochemical cycling. To develop LIBs of high energy density and high capacity, extensive research is being performed to develop new anode materials, including silicon and tin. The insertion of lithium into the active materials, such as graphite, silicon and tin, used in LIBs always results in rapid volume expansion, for example, which can reach to ~400% in silicon. The volume expansion in the active materials is known to be largely responsible for the stress evolution in electrodes; and a consequence of the stress evolution is structural degradation of the active materials which could rapidly lead to the failure of LIBs. The stress-induced-structural degradation has limited the use of bulk structural materials of high energy density and capacity in LIBs, and this has stimulated the research to develop structural materials of low-dimensions, such as thin films, nanowires, and nanoparticles, for LIBs.

Winter and Besenhard in their review paper [1] showed that the electrochemical lithiation of tin caused surface cracks and local delamination from the copper substrate, which eventually led to the loss of electronic contact. Maranchi et al. [2] observed the cracking and debonding of amorphous Si on the Cu-foil substrate, which were created by the insertion and de-insertion of lithium into silicon during electrochemical cycling. Uia et al. [3] investigated the electrochemical characteristics of Sn film as negative electrode for

lithium secondary batteries and observed the cracking of Sn film after the first discharge. Recently, Chao et al. [4] performed the in situ observation of the lithium insertion into Sn particles and revealed the formation of cracks in the lithiated layer during the first lithiation. Obviously, the microcracking and debonding during the lithium insertion and de-insertion present a challenge to the development of advanced LIBs for use in hybrid electric vehicles and plug-in hybrid electric vehicles.

As observed in experiments, there are two types of structural damage associated with the insertion of lithium into the active materials in LIBs; (1) microcracking and (2) debonding. To address the insertion-induced structural damage, Aifantis et al. [5] assumed a damaged layer existed over an active, elastic spherical particle and studied the propagation of cracks into the particle. Maranchi et al. [2] used the energy principle to analyze the debonding of amorphous silicon films from the Cu substrate, in which they did not consider the effect of the lithium concentration on the debonding behavior. Currently, little effort has been made to analyze the initiation condition of the microcracking and debonding from the viewpoint of the insertion-induced stress.

It is known that the prevention of the microcracking and debonding of thin films during the insertion and de-insertion of lithium determines the reliability and service life of LIBs. The understanding of the initiation of the microcracking and debonding plays an important role in the structural design and material selection of the next-generation LIBs. It is the purpose of this work to use the energy principle to study the initiation of the microcracking and debonding of an elastic film on a rigid substrate. In contrast to the work reported in literature, the theory of diffusion-induced stress is used in the analysis. Simple relations are derived between the size of the cracking/debonding of the film and the concentration of solute atoms, which provide an upper limit of the lithium concen-

* Tel.: +1 8592572994; fax: +1 8593231929.
E-mail address: fyang0@engr.uky.edu.

tration used in LIBs for potentially mitigating the structural damage created by the lithium insertion.

2. Physical model

Consider an elastic film deposited on a rigid substrate. For generalization, we focus on the stress evolution created by the insertion of solute atoms into the film instead of limiting the study to the insertion of lithium. The insertion of solute atoms into the film introduces local volumetric expansion and mechanical stress, which can create through-thickness cracks and local debonding at the film–substrate interface. In general, both structural damage can occur simultaneously and result in structural failure. Fig. 1 illustrates these two types of structural damage caused by the insertion of solute atoms, in which the film experiences compressive stress. The compressive stress consists of the insertion-induced stress and the residual stress created externally during the processing and handling, which can either create local surface cracking or cause local debonding/buckling. This eventually leads to structural failure of the film during the insertion process.

The principle of the insertion-induced stress is similar to that of the diffusion-induced stress, which was originally analyzed by Prussin [6]. Li [7] studied the diffusion-induced stress in elastic materials of simple geometries. Lee and co-workers [8,9] analyzed the effect of diffusion on the stress evolution in composite materials. Yang and Li [10] considered the effect of chemical stress on the bending of simple beam/plate structures. Yang [11] established a new relation between hydrostatic stress and the concentration of solute atoms in studying the interaction between chemical stress and diffusion. Recently, Yang [12] incorporated the volumetric change due to local solid reaction in the theory of the diffusion-induced stress and developed a general relation among the concentration of solute atoms, local reaction product, and mechanical stress. However, the study only focused on the deformation of elastic materials.

From the theory of diffusion-induced stress [7,11], the stress–strain relationship for the insertion-induced stress in an isotropic and homogeneous elastic film can be expressed as

$$\varepsilon_{ij} = \frac{1}{E}[(1+\nu)\sigma_{ij} - \nu\sigma_{kk}\delta_{ij}] + \frac{C\Omega}{3} \tag{1}$$

where ε_{ij} and σ_{ij} ($i, j = 1, 2, 3$) are the components of strain tensor and stress tensor, respectively, Ω is the coefficient of the volume expansion per mole of solute atoms ($m^3 mol^{-1}$), and C is the concentration ($mol m^{-3}$) of solute atoms, E and ν are Young's modulus and Poisson's ratio of the film, respectively. For simplicity, only one-dimensional compression in the x-direction is considered in the following analysis.

For one-dimensional compression in the x-direction, the non-zero components of stress tensor and strain tensor are σ_{xx} and ε_{xx}, respectively. Using the results for the thermal stress in an elastic film [13], one obtains the resultant in-plane stress in the film with a uniform distribution of solute atoms as

$$\sigma_{xx} = \frac{E}{1-\nu}\left(\varepsilon_0 - \frac{1}{3}C\Omega\right) \tag{2}$$

where ε_0 is the mismatch strain at the film–substrate interface, which is created during the processing and handling of LIBs. The mismatch strain of ε_0 can create either tensile stress or compressive stress in the film. For $\varepsilon_0 < 0$, a compressive stress is generated in the film similar to the stress state of the electrodes in conventional LIBs, which is created from the cell/pack packaging.

The strain energy density, U_E, stored in the film is then calculated from Eq. (2) as

$$U_E = \frac{1}{2}\sigma_{xx}\varepsilon_{xx} = \frac{E}{2(1-\nu)}\left(\varepsilon_0 - \frac{1}{3}C\Omega\right)^2 \tag{3}$$

For $\varepsilon_0 = 0$, i.e. the incoherent interface between the film and the substrate or the film initially being at a stress-free state, Eq. (3) gives

$$U_E = \frac{E(C\Omega)^2}{18(1-\nu)} \tag{4}$$

The strain energy density is proportional to the square of the concentration of solute atoms in the film.

3. Results and discussion

3.1. Surface cracking

Consider the formation of surface cracks in the elastic film. Assume that the cracking process is adiabatic and there is no kinetic energy involved in the cracking process. For the formation of an array of parallel-through-thickness, straight cracks with an average distance of l_c between them, each surface crack creates two new surfaces; and the stress in the film is relaxed through the increase in surface energy. For a slow cracking process to form a pair of parallel cracks, the decrease in total energy requires

$$l_c h U_E \geq 2h\gamma_1 \tag{5}$$

where γ_1 is the surface energy of the film. Substituting Eq. (3) into Eq. (5), one obtains

$$\varepsilon_{xx} \geq 2\sqrt{\frac{1-\nu}{E}\frac{\gamma_1}{l_c}} \tag{6}$$

which gives the critical concentration for the initiation of surface cracks, $C_{cr}^{(c)}$, as

$$C_{cr}^{(c)} = \frac{3}{\Omega}\left(2\sqrt{\frac{\gamma_1}{l_c}\frac{1-\nu}{E}} + \varepsilon_0\right) \tag{7}$$

The critical concentration of solute atoms is independent of the film thickness and is inversely proportional to the square root of
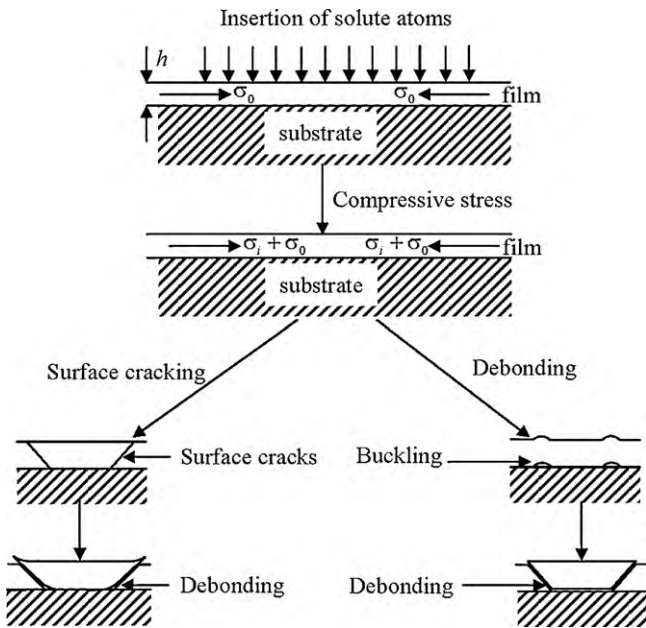

Fig. 1. Schematic diagram showing the structural damage created by the insertion of solute atoms into an elastic film (σ_0 is the compressive stress applied externally, and σ_i is the insertion-induced stress).

the average distance between surface cracks. The smaller the concentration of solute atoms is, the larger the distance between the surface cracks created by the insertion of solute atoms is as well. The insertion of high concentration of solute atoms into the elastic film will create dense surface cracks, which can readily cause structural damage to the film during the insertion process.

As given in Eq. (7), the critical concentration of solute atoms is a linear function of the mismatch strain. For an elastic film initially subject to an in-plane compressive mismatch strain/stress, i.e. $\varepsilon_0 < 0$, it needs less concentration of solute atoms than that for a stress-free film to create similar types of surface cracks.

3.2. Local buckling

Various theories of the buckling of elastic plates under the action of in-plane compressive stress have been established. The analyses have shown that local buckling will occur when the compressive stress in an elastic film reaches a critical stress [14]. In contrast to the study of the compression-induced buckling of elastic beams and plates, there is little research available on the insertion-induced buckling of elastic structures.

In general, the insertion-induced buckling of a surface film deposited on a rigid substrate also involves the separation of the film from the substrate. Thus, part of the strain energy in an unbuckled film is relaxed through the formation of two new surfaces from the film–substrate interface, and the other is stored in the buckled film. From the energy principle, the condition for the formation of the insertion-induced buckling of an elastic film in a strip shape of size l_d is

$$l_d h U_E \geq l_d \Delta\gamma + l_d h U_B \tag{8}$$

The parameter of $\Delta\gamma$ is the Dupré constant, which is defined as

$$\Delta\gamma = \gamma_1 + \gamma_2 - \gamma_{12} \tag{9}$$

Here, γ_2 is the surface energy of the substrate, and γ_{12} is the interface energy for the film–substrate interface. The term on the left side of Eq. (8) is the total strain energy stored in the elastic strip before the occurrence of the delamination, the first term on the right side of Eq. (8) represents the surface energy due to the formation of two new surfaces, and the second term on the right side of Eq. (8) is the strain energy stored in the buckled strip after the delamination and buckling.

The parameter of U_B is the strain energy density stored in the buckled film, which can be calculated from the result given by Gille and Rau [15] from the plate theory as

$$U_B = \frac{\pi^2}{24} \left(\frac{h}{l_d}\right)^2 \frac{E\varepsilon_{xx}}{1 - \nu^2} \tag{10}$$

Substitution of Eqs. (3) and (10) into Eq. (8) yields

$$\varepsilon_{xx}^2 \geq \frac{2(1-\nu)}{E} \frac{\Delta\gamma}{h} + \frac{\pi^2}{12} \left(\frac{h}{l_d}\right)^2 \frac{\varepsilon_{xx}}{1+\nu} \tag{11}$$

which gives

$$\varepsilon_{xx} \geq \frac{\pi^2}{24} \frac{1}{1+\nu} \left(\frac{h}{l_d}\right)^2 + \sqrt{\frac{2(1-\nu)\Delta\gamma}{Eh} + \frac{1}{(1+\nu)^2} \left(\frac{\pi^2}{24}\right)^2 \left(\frac{h}{l_d}\right)^4} \tag{12}$$

i.e.

$$\frac{1}{3} C\Omega \geq \frac{\pi^2}{24} \frac{1}{1+\nu} \left(\frac{h}{l_d}\right)^2$$
$$+ \sqrt{\frac{2(1-\nu)\Delta\gamma}{Eh} + \frac{1}{(1+\nu)^2} \left(\frac{\pi^2}{24}\right)^2 \left(\frac{h}{l_d}\right)^4} + \varepsilon_0 \tag{13}$$

For $\Delta\gamma = 0$, the critical strain determined from Eq. (12) is the same as that for the buckling of an elastic plate by uniaxial compression [14]. In contrast to the insertion-induced surface cracking, the buckling of the film created by the insertion of solute atoms is dependent upon the delamination size and the Dupré constant. It is worth noting that Eq. (10) is slightly different from the result given by Gille and Rau [15]. The constant in the Eq. (6) of Gill and Rau's paper is determined by matching the result for the buckling of an elastic plate under the action of an in-plane compressive stress.

From Eq. (13), the critical concentration for the initiation of the insertion-induced buckling, $C_{cr}^{(b)}$, is found as

$$C_{cr}^{(b)} = \frac{3}{\Omega} \left[\frac{\pi^2}{24} \frac{1}{1+\nu} \left(\frac{h}{l_d}\right)^2 \right.$$
$$\left. + \sqrt{\frac{2(1-\nu)\Delta\gamma}{Eh} + \frac{1}{(1+\nu)^2} \left(\frac{\pi^2}{24}\right)^2 \left(\frac{h}{l_d}\right)^4} + \varepsilon_0 \right] \tag{14}$$

which is a function of the film thickness. As given in Eqs. (7) and (14), it needs a relatively small amount of solute atoms to cause structural damage in an elastic film, including surface cracking and local buckling, during the insertion when the film is initially subjected to a compressive mismatch strain/stress, $\varepsilon_0 < 0$. Both critical concentrations are inversely proportional to the coefficient of the volume expansion. The smaller the coefficient of the volume expansion is, the larger the critical concentration for the occurrence of the insertion-induced structural damage is as well. In addition, Eqs. (7) and (14) provide a possible approach to measure the surface/interface energy from the insertion-induced surface cracking or buckling.

3.3. Numerical calculation

As discussed previously, extensive research has been conducted to develop low-dimensional materials for the applications in LIBs. Here, we consider the insertion of lithium into a tin film of 100 nm, which is coated on the surface of a cast iron with an incoherent interface, i.e. $\varepsilon_0 = 0$. The mechanical properties of tin are $E = 45$ GPa [16] and $\nu = 0.33$ [17]. The surface energies of tin and cast iron are $0.7 \, J\,m^{-2}$ [18] and $2.40 \, J\,m^{-2}$ [19], respectively. There is no data available for the interface energy of the planar Sn/Fe interface. In the calculation, the average value of the surface energy of tin and the surface energy of cast iron is used as the interface energy of the Sn/Fe interface, i.e. $\gamma_{12} = 1.55 \, J\,m^{-2}$, as an approximation.

Fig. 2 shows the dependence of the critical concentration of lithium on the average damage size of l (i.e. l_c or l_d). The critical con-
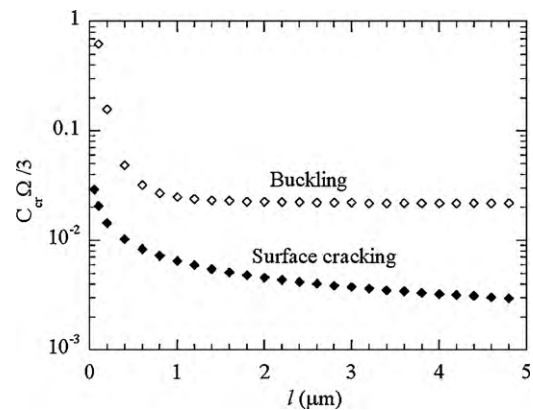

Fig. 2. Dependence of the critical concentration of lithium on the average damage size.
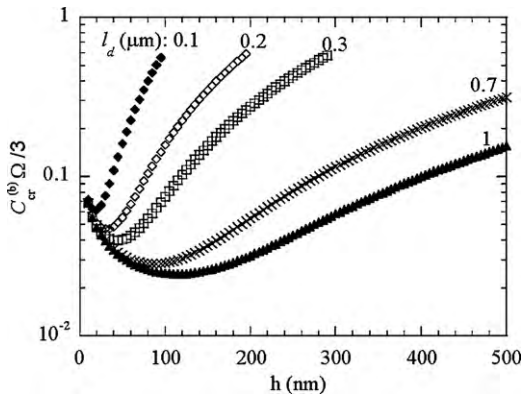
Fig. 3. Variation of the critical concentration of lithium with the film thickness for various buckling sizes.

centration varies nonlinearly with the average damage size. Small concentration of lithium will cause less structural damage to the tin film than that caused by high concentration of lithium, as expected. To prevent the structural degradation during the charging and discharging of LIBs, a compromise needs to be made between the magnitude of the charging current and the lifetime of LIBs.

It is interesting to note that the insertion-induced formation of surface cracks in the tin film requires less concentration of lithium than that for the formation of local delamination/buckling. This result suggests that structural damage due to surface cracking occurs much easier than that due to local delamination/debonding for the same concentration of lithium, which is in good accord with some experimental observation. Surface cracking of films always occurs first during electrochemical cycling for lithium-ion-based electrochemical systems [2–4].

Fig. 3 shows the effect of the film thickness on the critical concentration of lithium for various delamination sizes of local debonding created by the insertion of lithium into the tin film. For the same delamination size, the critical concentration first decreases with the film thickness to a minimum, and then increases with the film thickness. Such a behavior is related to the energy released during local delamination and buckling. For ultrathin films ($h/l_d \ll 1$), most of the strain energy is released through the creation of two new surfaces, while, for thick films, most of the strain energy is released by decreasing the stress in the film through local buckling.

Using Eq. (14) and taking the first derivative of the critical concentration with the film thickness, one obtains the film thickness corresponding to the minimum critical concentration for a given buckling size and the minimum critical concentration, $\mathrm{Min}(C_{cr}^{(b)})$, as

$$h^5 = \frac{3\Delta\gamma l_d^4(1+\nu)}{E}\left(\frac{2}{\pi}\right)^4 \tag{15}$$

and

$$\mathrm{Min}(C_{cr}^{(b)}) = \frac{9}{\Omega(1+\nu)}\left(\frac{2}{23}\right)^{3/5}\left(\frac{\pi(1-\nu^2)^2}{1-\nu}\frac{\Delta\gamma}{l_d E}\right)^{2/5} \tag{16}$$

The minimum critical concentration is determined by the ratio of $\Delta\gamma/l_d E$. For a given concentration of solute atoms and the film–substrate system, one can use Eq. (16) to estimate the largest size of the local delamination created by the insertion of solute atoms.

Recently, several groups have reported that Young's modulus of thin films decreases with the decrease of the film thickness for Ta/Cu/Ta films of thickness less than 300 nm [20] and Pd films of thickness less than 200 nm [21]. One expects that other thin films will likely have similar behavior, i.e. Young's modulus decreases

with the decrease of the film thickness. According to Eq. (7) and the results shown in Fig. 2, the critical concentration for the initiation of surface cracks will increase with the decrease of Young's modulus. This indicates that there is less possibility for ultrathin films to experience the surface cracking created by the insertion of solute atoms than thick films for the same concentration of solute atoms. Ultrathin films have higher electrochemical durability than thick films and are preferred for the applications in LIBs if structural durability is a major concern. For the insertion-induced buckling, it is the Eh that determines the size effect of elasticity on the critical concentration for structural durability. Obviously, more work needs to be done to examine the size-dependence of the mechanical behavior of thin films for understanding the structural durability of the materials and structures used in LIBs.

Currently, most LIBs use composite porous electrodes, which consist of active materials and binder and complicate the analysis of structural durability. For composite porous electrodes, the material properties, such as Young's modulus and the coefficient of volumetric expansion, become a function of compositions and porosity. One can use the law of mixture to make an approximate calculation or the homogenization model to calculate apparent material properties. This requires the measurement of the material properties of each composition or the direct measurement of the material properties of the composites. In addition, surface cracking can be initiated along the interface between binder and active materials, along the interface between active particles, or through particles and binders; and local buckling/debonding can occur along the interface between binder and the electrode substrate or along the interface between active materials and the electrode substrate. This makes it necessary to experimentally or theoretically determine the bonding strength between individual phases in order to use Eqs. (7) and (14) to approximately estimate the critical concentration of solute atoms for possible mitigation of local structural degradation in composite porous electrodes.

4. Conclusion

The energy principle is basic to the analysis and prediction of the structural damage involving the insertion/diffusion of solute atoms, such as the insertion-induced stress and damage in LIBs. The effect of the interaction between stress and insertion/diffusion on structural degradation cannot be simply described by a limiting process on the macroscopic level. However, the requirement of the reduction in system energy has significant consequence in determining the cracking and buckling behavior of materials created by the volumetric change due to the insertion of solute atoms.

The work presented here has attempted to bring out the potential importance of the insertion-induced deformation in examining the structural damage resulting from the mechanical deformation of materials. In particular, the study has shown that one can use the energy principle to obtain the upper limit of the concentration of solute atoms, which creates structural damage in thin films from the framework of elasticity. For the surface cracking in thin films, the critical concentration is independent of the film thickness, while it is a linear function of the square root of the surface energy of the films and the inverse of the square root of Young's modulus of the films. Thin films with lower Young's modulus than that for thick films have relatively good structural durability in controlling the surface cracking. For the local buckling/delamination, the structural durability is dependent on the ratio of the Dupré constant to the parameter of Eh. These results are applicable to any case involving diffusion- or insertion-induced structural failure in the limit of elasticity. They can be applied not only to the structural damage of thin films created by the lithium insertion in LIBs but also to the

structural damage of thin films created by hydrogen diffusion in fuel cells.

The present analysis provides a first step to examine the structural durability of thin films in electrochemical environment for potential applications in LIBs. Due to the complex structures of the composite porous materials currently used in LIBs, one needs to use numerical simulation and the concept developed in this work to further analyze the conditions for surface cracking and local buckling.

Acknowledgment

References

[1] M. Winter, J.O. Besenhard, Electrochim. Acta 45 (1999) 31–50.
[2] J.P. Maranchi, A.F. Hepp, A.G. Evans, N.T. Nuhfer, P.N. Kumta, J. Electrochem. Soc. 153 (2006) A1246–A1253.
[3] K. Uia, S. Kikuchia, Y. Kadomaa, N. Kumagai, S. Ito, J. Power Sources 189 (2009) 224–229.
[4] S.-C. Chao, Y.-C. Yen, Y.-F. Song, Y.-M. Chen, H.-C. Wu, N.-L. Wu, Electrochem. Commun. 12 (2010) 234–237.
[5] K.E. Aifantis, S.A. Hackney, J.P. Dempsey, J. Power Sources 165 (2007) 874–979.
[6] S. Prussin, J. Appl. Phys. 32 (1961) 1876–1881.
[7] J.C.M. Li, Metall. Trans. A 9A (1978) 1353–1380.
[8] S.B. Lee, W.L. Wang, J.R. Chen, Mater. Chem. Phys. 64 (2000) 123–130.
[9] W.L. Wang, S.B. Lee, J.R. Chen, J. Appl. Phys. 91 (2002) 9584–9590.
[10] F.Q. Yang, J.C.M. Li, J. Appl. Phys. 11 (2003) 9304–9309.
[11] F.Q. Yang, Mater. Sci. Eng. A409 (2005) 153–159.
[12] F.Q. Yang, J. Appl. Phys. 107 (2010) 103516.
[13] J.-H. Jou, L.-J. Chen, Appl. Phys. Lett. 59 (1991) 46–47.
[14] S.P. Tomoshenko, J.M. Gere, Theory of Elastic Stability, McGraw-Hill Book Company, Inc., New York, 1961.
[15] C. Gille, B. Rau, Thin Solid Films 120 (1984) 109–112.
[16] T. El-Ashram, Radiat. Effects Defects Solids 161 (2006) 193–197.
[17] B.-Z. Lee, D.N. Lee, Acta Mater. 46 (1998) 3701–3714.
[18] P.L. Clavette, Tin Whisker Growth in Electronics, Master Project, Rensselaer Polytechnic Institute, Hartford, Connecticut, 2009.
[19] S. Hong, Curr. Appl. Phys. 3 (2003) 457–460.
[20] K. Fujiwara, H. Tanimoto, H. Mizubayashi, Mater. Sci. Eng. A 442 (2006) 336–341.
[21] S.U. Jen, T.C. Wu, Thin Solid Films 492 (2005) 166–172.